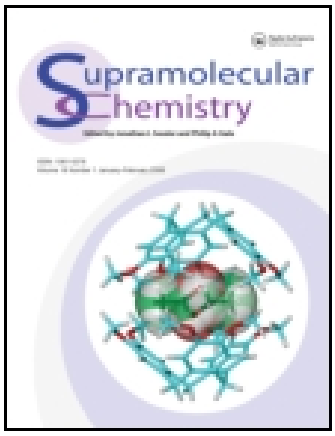

Supramolecular Chemistry
Publication details, including instructions for authors and subscription information:
http://www.tandfonline.com/loi/gsch20

Multi-Component Synthesis of Tetracavitand Nanocapsules

Xuejun Liu [a] , Yong Liu [a] , [b] & Ralf Warmuth [a]

[a] Rutgers, The State University of New Jersey, Department of Chemistry and Chemical Biology , Piscataway, NJ, 08854, USA

[b] Early Development Analytical Research, Merck Research Laboratories , Rahway, NJ, 07065, USA

Published online: 03 Apr 2008.

To cite this article: Xuejun Liu , Yong Liu , & Ralf Warmuth (2008) Multi-Component Synthesis of Tetracavitand Nanocapsules, Supramolecular Chemistry, 20:1-2, 41-50, DOI: 10.1080/10610270701742546

To link to this article: http://dx.doi.org/10.1080/10610270701742546

Supramolecular Chemistry, January–March 2008 Vol. 20 (1–2), pp. 41–50

Multi-Component Synthesis of Tetracavitand Nanocapsules

XUEJUN LIU[a], YONG LIU[a,b] and RALF WARMUTH[a]*

[a]*Department of Chemistry and Chemical Biology, Rutgers, The State University of New Jersey, Piscataway, NJ 08854, USA;* [b]*Merck Research Laboratories, Early Development Analytical Research, Rahway, NJ 07065, USA*

(Received 2 August 2007; Accepted 11 October 2007)

The syntheses of three hexadecaimino nanocapsules 4b–d via the trifluoroacetic acid-catalysed condensation of four equivalents of a tetraformylcavitand 2 with eight equivalents of 1,4-phenylenediamine 3b, benzidine 3c or 4,4′-ethylenedianiline 3d, respectively, are reported. These nanocapsules are shaped like a tetragonal tetrahedron and have solvodynamic diameters of 2.5–3 nm, which were estimated from their diffusion constants. The smallest of these tetragonal tetrahedra 4b, which has a cavity volume of 1250 Å^3, forms 1:1 and 2:1 complexes with $R_4N^+Br^-$ salts (R = *n*-pentyl, *n*-hexyl, *n*-heptyl) in organic solvents. Complexation-induced shifts and the slow exchange rates between the free and complexed guests are consistent with the guest being fully encapsulated inside the nanocapsule.

Keywords: Dynamic covalent chemistry; Nanocapsule; Host–guest chemistry; Encapsulation; Molecular container molecule

INTRODUCTION

Molecular container compounds offer new interesting opportunities in chemical and biological sciences [1–7]. They have shown great promise as nanoreactors [8,9], in which fleeting intermediates are stabilised [10–15] and reaction rates [16–18], regio- and stereochemistry are altered [19–21], as building blocks for nanodevice fabrication [22, 23], and in delivery [24], storage and separation technology [25]. Container molecules that are large enough to encapsulate multiple guest molecules also allow probing of weak intermolecular interactions between these guests [6, 26–28]. In recent years, highly efficient self-assembly processes utilising hydrogen bonding or metal coordination chemistry have been developed for the multicomponent synthesis of large molecular capsules [4–7, 29–40]. Self-assembly provides a proofreading and error correction mechanism and typically yields the desired nanocapsule quantitatively, provided that it is the thermodynamically most stable assembly. The same virtues are inherent to dynamic covalent chemistry (DCC), in which reactants are linked by dynamic covalent bonds that form reversibly under the correct reaction conditions [41]. DCC has been applied successfully for the synthesis of dynamic combinatorial libraries [42–44], responsive materials [45–47], topologically and structurally highly complex molecules [48–50] and molecular container compounds [51–56]. For example, octaimine hemicarcerands **1e–h** are the only observable products in the acid-catalysed condensation of two equivalents of tetraformylcavitand **2** with four equivalents of diamines, such as 1,3-phenylenediamine **3e**, propane-1,3-diamine **3f**, butane-1,4-diamine **3 g** or pentane-1,5-diamine **3 h** (Chart 1) [51–55]. We recently discovered that this condensation leads to larger nanocapsules, whose size and shape are solvent dependent, if ethylene-1,2-diamine **3a** is the diamine building block [53–55]. In chloroform, this reaction yields an octahedral nanocapsule **5** composed of 6 cavitands and 12 ethylenediamines [54,55]. On the other hand, the tetragonal tetrahedron **4a** or the square antiprism **6** are the major products in tetrahydrofuran or dichloromethane, respectively (Scheme 1) [53].

The lack of formation of hemicarcerand **1a** is likely a consequence of higher conformational energy of the 1,2-diaza-ethylene linkers in **1a**, which require a *gauche* conformation as apposed to **4a**, **5**–**6**, in which an *anti* conformation is possible. Thus, our hypothesis has been that linear diamines, in which the angle between the C—N bonds is 180° in the lowest energy conformation, have the propensity to yield larger nanocapsules and those, whose angles are

*Corresponding author. E-mail: warmuth@rutgers.edu

ISSN 1061-0278 print/ISSN 1029-0478 online © 2008 Taylor & Francis
DOI: 10.1080/10610270701742546

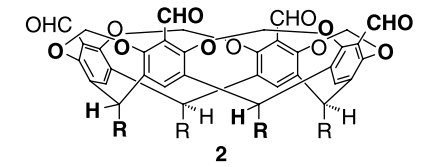

2

$H_2N–X–NH_2$

R = pentyl

3a-h

suffix	X
a	$-CH_2-CH_2-$
b	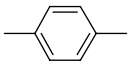
c	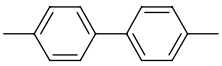
d	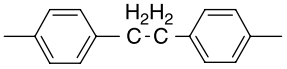
e	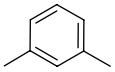
f	$-CH_2-CH_2-CH_2-$
g	$-CH_2-CH_2-CH_2-CH_2$
h	$-CH_2-CH_2-CH_2-CH_2-CH_2$

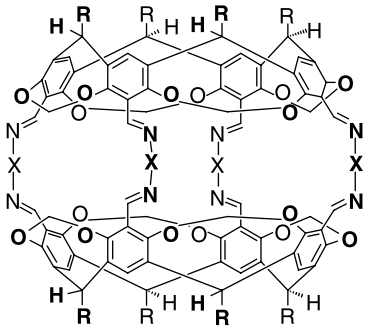

1a-h

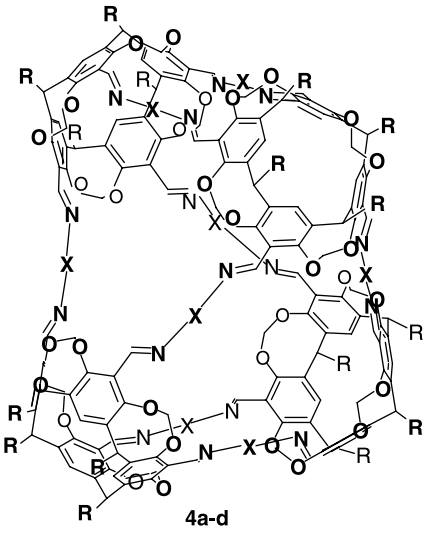

4a-d

CHART 1

around 120°, preorganise linked cavitands for further growth into an octaimine hemicarcerand [53]. Here, we address the question whether other, more rigid linear diamines will yield related tetrameric, hexameric and/or octameric nanocapsules that were observed with **3a**. For this investigation, we choose diamines **3b–d**, which are more rigid than **3a**, whose conformational flexibility decreases in the order **3a** > **3d** > **3b** = **3c** and which might provide nanocapsules with a broad spectrum of cavity sizes.

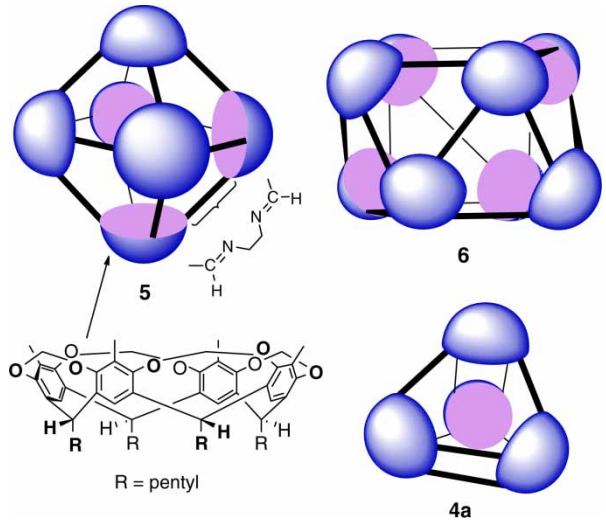

SCHEME 1 Nanocapsules assembled from cavitand **2** and ethylene-1,2-diamine.

EXPERIMENTAL SECTION

General Methods

All reactions were conducted under argon. Reagents and chromatography solvents were purchased from Aldrich and used without any further purification, except that chloroform was passed through K_2CO_3 prior to use. ^{1}H NMR spectra recorded in $CDCl_3$, toluene-d_8 or THF-d_8 were referenced to residual $CHCl_3$, $CHD_2C_6D_5$ and $(CHDCD_2CD_2CD_2)O$ at 7.26, 2.09 and 1.73 ppm, respectively. ^{13}C NMR spectra recorded in $CDCl_3$ or toluene-d_8 were referenced to $^{13}CDCl_3$ at 77.0 ppm and $^{13}CD_3C_6D_5$ at 20.8 ppm. Mass spectra were recorded on an Applied Biosystems Voyager DE-Pro mass spectrometer (MALDI-TOF). 2,4,6-Trihydroxyacetophenone was used as the matrix. Gel permeation chromatography

(GPC) was performed on a Thermo SpectraSYSTEM HPLC system equipped with dual wavelength UV/Vis detector (280 nm), Eppendorf CH-30 column heater and two Jordi GPC columns (cross-linked DVB, 10^3 Å pore size, MW cut-off ~ 25,000, 7.8 mm × 30 cm) with CH_2Cl_2/1% NEt_3 as the mobile phase at a flow of 1 ml/min. Approximate molecular weights of analytes were determined from a semi-logarithmic calibration plot (ln(MW) against retention time) using the following molecular weight standards: benzene (MW 78), cavitand **2** (MW 928), NMP hemicarceplex (MW 2348) [70] and three polyamino nanocapsules (MW 3941, 5912 and 7882) [53,54].

Synthesis of Hexadecaimino Nanocapsule 4b (Procedure A)

A solution of cavitand **2** (105.6 mg, 0.114 mmol), *para*-phenylenediamine **3b** (25.0 mg, 0.231 mmol) and CF_3CO_2H (TFA) (0.79 μl, 0.0107 mmol) in toluene (21.0 ml) was stirred for 0.5 h. Molecular sieves (3 Å) were added to the flask and stirring was continued overnight. The mixture was filtered and solid anhydrous K_2CO_3 was added to the filtrate. After stirring for 5 h, salts were filtered off. The filtrate was concentrated under reduced pressure and the yellow residue was dried at high vacuum overnight (121 mg, 99% yield, >95% purity based on ^{1}H NMR integration).

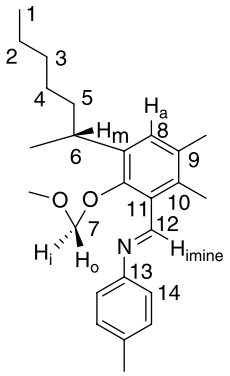

^{1}H NMR (500 MHz, toluene-d_8, 25°C), δ_H (ppm): 8.71 (s, 8H, H_{imine}), 8.28 (s, 8H, H_{imine}), 7.65 (s, 8H, H_a), 7.60 (s, 8H, H_a), 7.01 (s, 16H, H(14)), 6.73 (s, 16H, H(14)), 6.28 (d, J = 8.20 Hz, 4H, H_o), 5.99 (d, J = 7.80 Hz, 8H, H_o), 5.53 (t, J = 7.79 Hz, 4H, H_m), 5.37 (t, J = 8.20 Hz, 8H, H_m), 5.17 (d, J = 8.20 Hz, 4H, H_i), 5.14 (t, J = 7.79 Hz, 4H, H_m), 4.83 (d, J = 7.79 Hz, 8H, H_i), 4.01 (d, J = 7.38 Hz, 4H, H_o), 3.97 (d, J = 7.79 Hz, 4H, H_i), 2.49–2.26 (m, 32H), 1.54–1.25 (m, 96H), 0.92–0.88 (m, 48H, CH_3). ^{13}C NMR (125 MHz, toluene-d_8, 25°C), δ_C (ppm): 156.83 (C12), 156.77 (C12), 155.76 (C10), 155.57 (C10), 154.49 (C10), 154.31 (C12), 154.25 (C12), 153.72 (C10), 153.18 (C13), 151.76 (C13), 140.09 (C9), 140.08 (C9), 138.99 (C9), 138.86 (C9), 124.69 (C11), 124.66 (C11), 122.78 (C8), 122.56 (C8), 122.15 (C14), 121.74 (C14), 102.08 (C7), 101.35 (C7), 99.72 (C7), 37.33 (C6), 37.18 (C6), 37.03 (C6), 32.48 (C4), 32.34 (C4), 30.90 (C4), 30.44 (C5), 30.31 (C5), 30.04 (C5), 28.21 (C3), 28.16 (C3), 28.11 (C3), 23.24 (C2), 23.20 (C2), 23.18 (C2), 14.32 (C1), 14.31 (C1), 14.27 (C1). MALDI-TOF MS: m/z 4294.02 (100%, M + H^+; 4294.16 calcd for $C_{272}H_{289}N_{16}O_{32}$). GPC: t_R = 12.91 min (column temperature 25°C).

Synthesis of Hexadecaimino Nanocapsule 4c

From **2** (99.6 mg, 0.107 mmol), benzidine **3c** (40.3 mg, 0.219 mmol) and CF_3CO_2H (TFA) (0.8 μl, 0.0107 mmol) in chloroform (10.0 ml) according to *procedure A*. Deep yellow solid (121 mg, 92% yield, >95% purity based on ^{1}H NMR integration).

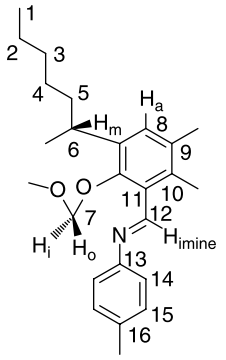

^{1}H NMR (500 MHz, $CDCl_3$, 25°C), δ_H (ppm): 8.66 (s, 8H, H_{imine}), 8.51 (s, 8H, H_{imine}), 7.61 (d, J = 8.30 Hz, 16H, C_6H_4), 7.54 (d, J = 8.30 Hz, 16H, C_6H_4), 7.29 (s, 8H, H_a), 7.28 (s, 8H, H_a), 7.19 (d, J = 8.30 Hz, 16H, C_6H_4), 7.06 (d, J = 8.30 Hz, 16H, C_6H_4), 5.91 (d, J = 7.64 Hz, 4H, H_o), 5.87 (d, J = 7.31 Hz, 8H, H_o), 5.46 (d, J = 6.97 Hz, 4H, H_o), 5.06–5.00 (m, 12H, H_m), 4.93 (t, J = 7.97 Hz, 4H, H_m), 4.82(d, J = 7.64 Hz, 4H, H_i), 4.75 (d, J = 7.31 Hz, 8H, H_i), 4.36 (d, J = 6.97 Hz, 4H, H_i), 2.31 (br s, 32H), 1.48–1.39 (m, 96H), 0.98–0.94 (m, 48H; CH_3). ^{13}C NMR (125 MHz, $CDCl_3$, 25°C), δ_C (ppm): 156.50 (C12), 155.36 (C12), 154.37 (C10), 154.22 (C10), 153.77 (C10), 152.89 (C10), 152.14 (C13), 151.80 (C13), 139.25 (C16), 138.96 (C16), 138.70 (C9), 138.50 (C9), 138.46 (C9), 138.26 (C9), 127.64 (C15), 127.52 (15), 124.10 (C11), 123.79 (C11), 122.27 (C8), 122.10 (C8), 121.48 (C14), 121.11 (C14), 100.67 (C7), 100.55 (C7), 99.67 (C7), 36.55 (C6), 36.44 (C6), 31.99 (C4), 31.96 (C4), 31.94 (C4), 29.93 (C5), 29.82 (C5), 29.51 (C5), 27.61 (C3), 27.59 (C3), 27.57 (C3), 22.73 (C2), 22.70 (C2), 14.11 (C1). MALDI-TOF MS: m/z 4902.62 (100%, M + H^+; 4902.41 calcd for $C_{320}H_{321}N_{16}O_{32}$). GPC: t_R = 12.54 min (column temperature 25°C).

Synthesis of Hexadecaimino Nanocapsule 4d

From **2** (110.2 mg, 0.119 mmol), 4,4′-ethylenedianiline **3d** (51.1 mg, 0.241 mmol) and CF_3CO_2H (TFA) (0.05 µl, 0.00067 mmol) in $CHCl_3$ (11.0 ml) according to *procedure A*. Reaction times: 2 h without and 1 h with 3 Å molecular sieves. Bright yellow solid (141 mg, 92% yield, >90% purity based on ^{1}H NMR integration).

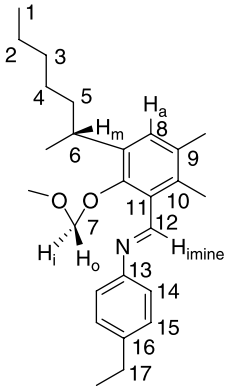

^{1}H NMR (400 MHz, $CDCl_3$, 25°C), δ_H (ppm): 8.60 (s, 8H, H_{imine}), 8.55 (s, 8H, H_{imine}), 7.29 (d, $J = 8.49$ Hz, 16H, C_6H_4), 7.27 (br s, 16H, H_a), 7.22 (d, $J = 8.29$ Hz, 16H, C_6H_4), 7.05 (d, $J = 8.19$ Hz, 16H, C_6H_4), 6.99 (d, $J = 8.10$ Hz, 16H, C_6H_4), 5.81 (d, $J = 7.51$ Hz, 12H, H_o), 5.71 (d, $J = 7.51$ Hz, 4H, H_o), 5.04–4.93 (m, 16H, H_m), 4.78 (d, $J = 7.71$ Hz, 4H, H_i), 4.71 (d, $J = 7.73$ Hz, 8H, H_i), 4.53 (d, $J = 7.06$ Hz, 4H, H_i), 2.90 (s, 32H, Ar-CH_2-), 2.31 (br s, 32H), 1.54–1.35 (m, 96H), 0.98–0.94 (m, 48H, CH_3). ^{13}C NMR (125 MHz, $CDCl_3$, 25°C), δ_C (ppm): 155.48 (C12), 155.14 (C12), 154.20 (C10), 154.05 (C10), 153.61 (C10), 153.14 (C10), 150.88 (C13), 150.57 (C13), 140.40 (C16), 140.06 (C16), 139.05 (C9), 138.91 (C9), 138.67 (C9), 138.53 (C9), 128.90 (C15), 128.81 (15), 124.13 (C11), 124.08 (C11), 122.06 (C8), 121.96 (C8), 120.98 (C14), 120.82 (C14), 100.65 (C7), 100.51 (C7), 100.06 (C7), 38.18 (C17), 37.39 (C17), 36.48 (C6), 36.44 (C6), 31.98 (C4), 31.96 (C4), 31.94 (C4), 29.89 (C5), 29.75 (C5), 29.63 (C5), 27.61 (C3), 27.57 (C3), 22.72 (C2), 22.71 (C2), 22.70 (C2), 14.10 (C1). IR (NaCl), ν (cm^{-1}): 2957, 2932, 2860, 1622, 1581, 1504, 1468, 1448, 1242, 1206, 1093, 958. MALDI-TOF MS: m/z 5126.15 (100%, M + H$^+$; 5126.66 calcd for $C_{336}H_{353}N_{16}O_{32}$). GPC: $t_R = 12.03$ min (column temperature 60°C).

Reduction of 4d

$NaBH_3CN$ in THF (1 M, 0.47 ml, 0.47 mmol) was added dropwise over 10 min to a mixture of tetramer **4d** (30.0 mg, 0.00585 mmol), $Ni(AcO)_2$ (25.7 mg, 0.103 mmol) in THF (14.6 ml). The mixture was stirred overnight at room temperature. The solvent was removed. The residue was stirred with 10 ml H_2O and 1 ml NH_3/H_2O for 20 min. It was extracted with 30 ml CH_2Cl_2. The organic layer was washed with 10 ml saturated $NaHCO_3$ (aq) and concentrated. The product was precipitated with methanol. The crude product was dried overnight at high vacuum at room temperature to yield an off-white solid. The solid was redissolved in 1 ml CH_2Cl_2 and precipitated with methanol. The precipitate was filtered off, washed with 3 × 1 ml methanol and dried overnight at high vacuum at room temperature. The crude product was purified by HPLC (PrincetonSPHER-300 Silica 300 Å, 5 µ, 150 × 4.6 mm, 1 ml/min, 280 nm, $t_R = 4.55$ min), which gave **7** as a white solid (23 mg; 72% yield based on cavitand **2** used for the synthesis of **4d**).

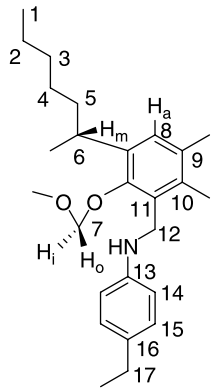

^{1}H NMR (300 MHz, $CDCl_3$, 25°C): $\delta = 7.22$ (s, 8H, H_a), 7.18 (s, 8H, H_a), 7.13 (d, $J = 8.49$ Hz, 16H, C_6H_4), 7.02 (d, $J = 8.49$ Hz, 16H, C_6H_4), 6.69 (d, $J = 8.38$ Hz, 16H, C_6H_4), 6.56 (d, $J = 8.38$ Hz, 16H, C_6H_4), 5.97 (d, $J = 6.95$ Hz, 4H, H_o), 5.91 (d, $J = 6.95$ Hz, 8H, H_o), 5.80 (d, $J = 6.95$ Hz, 4H; H_o), 4.89–4.81 (m, 16H, H_m), 4.46 (d, $J = 6.83$ Hz, 12H, H_i), 4.38 (d, $J = 6.37$ Hz, 4H, H_i), 4.19–4.11 (m, 16H, aryl-CH_2—N), 4.06 (d, $J = 10.76$ Hz, 8H, aryl-CHH—N), 3.98 (d, $J = 10.23$ Hz, 8H, aryl-CHH—N), 2.84–2.71 (m, 32H, Ar—CH_2—CH_2—Ar), 2.32–2.20 (m, 32H), 1.50–1.33 (m, 96H), 0.98–0.92 (m, 48H, CH_3). ^{13}C NMR (100.6 MHz, $CDCl_3$, 25°C), δ_C (ppm): 153.99 (C10), 153.82 (C10), 153.67 (C10), 146.56 (C13), 145.94 (C13), 138.60 (C9), 138.44 (C9), 138.20 (C9), 132.43 (C16), 132.17 (C16), 129.28 (C15), 129.00 (15), 125.42 (C11), 124.32 (C11), 120.07 (C8), 119.85 (C8), 114.05 (C14), 113.62 (C14), 100.39 (C7), 99.86 (C7), 99.67 (C7), 39.55 (C12), 38.71 (C12), 37.95 (C17), 37.67 (C17), 37.05 (C6), 32.03 (C4), 30.19 (C5), 27.62 (C3), 22.69 (C2), 14.10 (C1). MALDI-TOF MS: m/z 5159.07 (100%, M + H$^+$; 5159.92 calcd for $C_{336}H_{385}N_{16}O_{32}$).

DOSY Experiments

DOSY NMR experiments were performed on a 500 MHz Varian spectrometer equipped with a

gradient system that generates magnetic field pulse gradients in the *z*-direction of about 50 G/cm. A 5-mm broadband probe was used to carry out all the measurements. Samples were put into a 4-mm NMR tube that was inserted into a 5-mm NMR tube to reduce convection. Temperature was controlled at 298 K. Samples were equilibrated at least 10 min before the measurement started. The diffusion experiments were performed using the pulse sequence Dbppste (Bipolar Pulse Pair Stimulated Echo Experiment), which is implemented in the Varian VnmrJ software package. The diffusion delay (del, Δ) was set to 0.15 s. The gradient pulse strength (gzlvl1, G_z) was varied from 400 to 25,000 $(G/cm)^2$. For all other parameters, the default values were used. The diffusion rate constant (D) and its error reported in Table I are the mean average of the diffusion rate constants of each individual host proton signal in a D against δ plot and the SE of mean, respectively.

Binding Studies

Binding constants K for the encapsulation of tetraalkylammonium bromides inside the host **4b** were measured in THF-d_8 (or toluene-d_8) in the temperature range between 268 and 308 K. For all binding experiments, a 500 MHz Varian NMR spectrometer was used. NMR samples containing a known total host concentration ($[H]_0$) and total guest concentration ($[G]_0$) were equilibrated at least 10 min before each measurement. The 1:1 binding constants K were calculated from the integrals of the selected host, free guest and encapsulated guest signals according to the following equation: $K = [HG]/([H] \times [G]) = (I(G_{encap}CH_3)/12)/((I(H_{imine})/16 - I(G_{encap}CH_3)/12) \times ((I(G_{free}CH_2)/8)/(I(G_{free}CH_2)/8 + I(G_{encap}CH_3)/12)) \times [G]_0)$, where [H], [G] and [HG] are the concentrations of free host **4b**, free guest and complex, respectively, and $I(G_{encap}CH_3)$, $I(H_{imine})$ and $I(G_{free}CH_2)$ are the integrals of the 12 CH_3 protons of the encapsulated guest, the 16 imine protons of the host (free and complexed) and the eight α-CH_2 protons of the free guest, respectively. The enthalpy ΔH and entropy of complexation ΔS reported in Table III were determined from van't Hoff plots: $\ln(K) = \Delta S/R - \Delta H/R \times 1/T$).

TABLE I Diffusion constants D in $CDCl_3$ at 25°C and solvodynamic radii $r^{\dagger}$ of **4b–d**.

Nanocapsule	**4b**	**4c**	**4d**
D (10^{-10} m^2/s)	3.19 ± 0.05	2.77 ± 0.03	2.74 ± 0.02
r (Å)	12.7 ± 0.2	14.7 ± 0.2	14.8 ± 0.1

† $r = kT/6\pi\eta D$ with $\eta = 0.538$ mPa/s (*58*, *59*).

RESULTS AND DISCUSSION

Condensation of Tetraformylcavitand 2 with Diamines 3b–d

Addition of two equivalents of freshly sublimed **3b** to a solution of **2** in toluene containing 2.5 mol% trifluoroacetic acid (TFA) and activated molecular sieves gave a single condensation product as judged by the ^{1}H NMR spectrum and gel permeation chromatogram of the reaction mixture (Figs. 1 and 2). The addition of molecular sieves was important in order to drive the condensation reaction to completion by removing the formed water. The same product was also formed in chloroform and partially precipitated during the reaction. After removing the acid catalyst with solid potassium carbonate, the product was isolated in quantitative yield by solvent evaporation. We assign this product to the distorted tetrahedron **4b**. Our assignment is based on ^{1}H NMR, ^{13}C NMR spectra and MALDI-TOF MS spectra of **4b** and binding studies (*vide infra*), which show that **4b** is able to encapsulate one or two guest molecules, whose exchange with the free guest is slow on the NMR timescale. In the MALDI-TOF MS spectrum, the major ion has the correct mass-to-charge ratio $m/z = 4294.0$ expected for protonated **4b** ($[M + H]^+$, calcd $m/z = 4294.2$). Further support for **4b** comes from its ^{1}H NMR spectrum, as shown in Fig. 1. Consistent with the D_{2d} symmetry of **4b**, two sets of imine (H_{imine}), cavitand aryl (H_a) and linker aryl protons (H_l)—each with a ratio 8:8—and three sets of cavitand methine (H_m), inwards (H_i) and outwards pointing acetal protons (H_o)—each in a ratio 4:4:8—are observed.

The condensation reaction between four equivalents of **2** and eight equivalents of **3c** or **3d** gave tetrameric nanocapsules **4c** (quantitative) and **4d** (90% yield), respectively. Again, the assignment of these products to tetrahedral capsules was based on the similarity of their ^{1}H and ^{13}C NMR spectra to those of **4b**. The other products in the reaction of **3d** are small amounts of a trimer and hemicarcerand **1d**, which is supported by GPC and MALDI-TOF MS of the reaction mixture

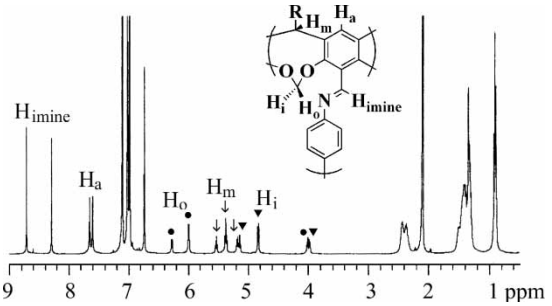

FIGURE 1 ^{1}H NMR spectrum (500 MHz, $C_6D_5CD_3$, 25°C of **4b**. Multiplets assigned to protons H_{imine}, H_i, H_o, H_a and H_m are marked.

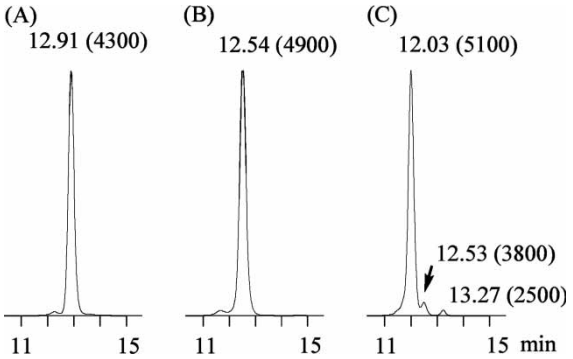

FIGURE 2 GPC traces of products in the TFA-catalysed condensation of four equivalents of **2** with eight equivalents of **3b** (A), **3c** (B) and **3d** (C). Retention time (min) and estimated molecular weight (in parentheses in Da) are given for each peak.

(Fig. 2). Reduction of all imine bonds of **4d** with $NaBH_3CN/Ni(OAc)_2$ in THF [56], or BH_3·THF followed by the hydrolysis of boramines with NaOH in methanol–THF gave polyamino nanocapsule **7**, which was separated from the other minor products by normal phase chromatography.

During these condensation reactions, we never observed hexameric or octameric nanocapsules, which were the major products in the reaction with ethylenediamine **3a**. Thus, linear diamines intrinsically prefer formation of a tetrameric nanocapsule and yield those exclusively, if they are rigid. We believe that enthalpic and entropic reasons contribute to this preference. In the cavitand building block, the angles between two C_{aryl}–$C_{carbonyl}$ bonds of opposite and adjacent aryl units are 61° and 56°, respectively, which are more appropriate to form a tetrahedron, but which are too small for a strain-free octahedron or square antiprism. However, even if tetrameric, hexameric and octameric products are equally strained, entropy will favour the smallest capsule (tetramer), which has the highest ratio of the intramolecular to intermolecular bonds (tetramer, 5:11; hexamer, 7:17; octamer, 9:23). Therefore, our design principle (cavitand + diamine) can only produce hexameric or octameric nanocapsules, if the smaller capsules (tetramer **4** or hemicarcerand **1**) are disfavoured enthalpically, e.g. via a high strain energy. The high strain energy is clearly the reason why hemicarcerands **1b–d** are not observed or only as a minor product (**1d**, <5% yield).

Diffusion Rate of Nanocapsules

The size of nanocapsules **4b–d** was estimated from their diffusion rate constants in $CDCl_3$, which were measured by DOSY NMR experiments (Table I) [57]. Application of the Stokes–Einstein equation yielded solvodynamic radii *r* for **4b–d**, which range from 12.7 to 14.8 Å (Table I) and which are consistent with energy-minimised structures of these capsules (Fig. 3). For example, the average distance between

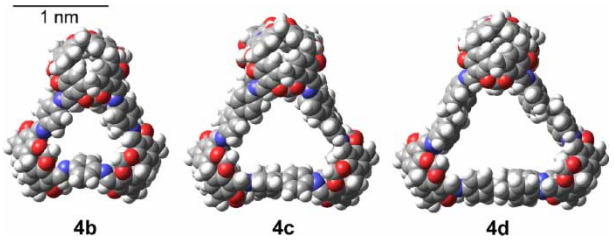

FIGURE 3 Energy-minimised space-filling models of nanocapsules **4b–d** (MM3 (*60*), gas phase). Pentyl groups are replaced with hydrogens. Atom colouring: C, grey; O, red; N, blue; H, white.

the centre of the cavity and the centre of each cavitand of **4c** is also approximately 2 Å longer (12.3 Å) when compared with the same average distance in **4b** (9.7 Å), suggesting that these nanocapsules have similar structures in solution.

Encapsulation of Tetraalkylammonium Bromides inside Nanocapsule 4b

Preliminary binding studies with **4b**, which has a cavity volume of approximately 1250 $Å^3$ [61], show 1:1 and 2:1 complexation of medium-sized tetraalkylammonium bromides. Addition of excess (n-$C_6H_{13})_4NBr$ or (n-$C_7H_{15})_4NBr$ to solutions of **4b** led to the appearance of a new set of strongly upfield-shifted signals, which are assigned to the encapsulated guests being in slow exchange with the free tetraalkylammonium bromides (Fig. 4; Table II) [62]. Based on integration, one guest molecule is encapsulated inside **4b**. Complexation was further supported by the observation of signals for ions

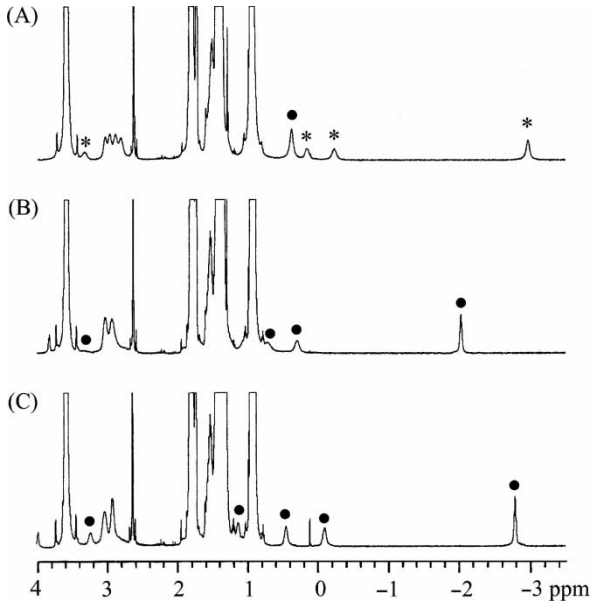

FIGURE 4 Partial ^1H NMR spectra (500 MHz, THF-d_8, 278 K) of **4b** in the presence of 20 equivalents of (n-$C_5H_{11})_4NBr$ (A), (n-$C_6H_{13})_4NBr$ (B) or (n-$C_7H_{15})_4NBr$ (C). Signals assigned to protons of the encapsulated guests of 1:1 and 2:1 complexes are marked with filled circles and asterisks, respectively.

TABLE II Complexation-induced shift of guest protons for complexes **4b**⊙$R_4N^+Br^-$ and **4b**⊙2($pentyl_4N^+Br^-$) in THF-d_8 at −5°C, guest's van der Waals volume V_G (*62c*) and packing coefficient PC.

Guest	V_G (Å^3)	PC	$\Delta\delta(H_1)$	$\Delta\delta(H_2)$	$\Delta\delta(H_3)$	$\Delta\delta(H_4)$	$\Delta\delta(H_5)$	$\Delta\delta(H_6)$	$\Delta\delta(CH_3)$
(n-C_5H_{11})$_4$NBr	383	0.31	0.26	n.d.	1.25	1.63			3.9
2 × (n-C_5H_{11})$_4$NBr	766	0.61	n.d.	n.d.	n.d.	0.45			0.55
(n-C_6H_{13})$_4$NBr	448	0.36	0.26	n.d.	n.d.	0.68	1.1		2.94
(n-C_7H_{15})$_4$NBr	514	0.41	0.4	0.35	n.d.	0.3	0.84	1.38	3.65

n.d., not determined; PC = V_G/V_{cavity}; V_{cavity} = volume of inner cavity of **4b** = 1250 Å^3 [61].

TABLE III Thermodynamic properties (ΔG_{298}, ΔH_{298} and $T\Delta S_{298}$ at 298 K in kcal/mol) of complexes **4b**⊙R_4NBr

Guest	Solvent	ΔG_{298}	ΔH_{298}	$T\Delta S_{298}$	K_1 (M^{-1})
(n-C_6H_{13})$_4$NBr	THF-d_8	−2.3	−6.6	−4.3	45 ± 5
(n-C_7H_{15})$_4$NBr	THF-d_8	−2.5	−6.9	−4.4	69 ± 7
(n-C_7H_{15})$_4$NBr	toluene-d_8	−4.6	1.3	5.9	2500 ± 200
(n-C_7H_{15})$_4$NBr	$CDCl_3$	n.c.	n.c.	n.c.	n.c.
(n-C_8H_{17})$_4$NBr	THF-d_8	n.c.	n.c.	n.c.	n.c.

n.c., no complexation; K_1 at 298 K; K_1 = [**4b**⊙R_4NBr]/[**4b**] [R_4NBr].

[**4b**⊙R_4N]$^+$ in the MALDI-TOF mass spectra of these solutions (Appendix A). Encapsulation of tetraoctylammonium bromide was not observed. However, strong downfield shifts of the aryl protons of the cavitands and $CH_2(CH_2)_3CH_3$ protons of the pentyl groups suggest that tetraoctylammonium ions bind to the outside of the cavitands of **4b**.

Upon addition of (n-C_5H_{11})$_4$NBr to **4b**, two sets of upfield-shifted guest signals are observed (Fig. 4A). We assign the set with the strongest upfield-shifted CH_3 group at $\delta = -2.96$ to the guest in the 2:1 complex and the set with the CH_3 signal at $\delta = 0.40$ to the guest in the 1:1 complex, since the ratio of the methyl proton integrals I(CH_3-2:1 complex)/I(CH_3-1:1 complex) increases with increasing guest concentration. Complexation of one and two guests was further supported by MALDI-TOF MS through the observation of ions with a mass-to-charge ratio calculated for [**4b**⊙$pentyl_4N$]$^+$ and [**4b**⊙($pentyl_4N$)$_2$-Br]$^+$ (Appendix A), and the ROESY spectrum which shows exchange peaks between the CH_3 signals of the free and encapsulated guests and between the CH_3 signals of the encapsulated guests in the 1:1 and 2:1 complexes. Both guests in the 2:1 complex must be encapsulated inside **4b**, since their protons are considerably upfield shifted and exchange with free (n-C_5H_{11})$_4$NBr has a free energy barrier greater than 13.5 kcal/mol.

Binding constants for all 1:1 complexes were calculated from the integrals of the methyl protons of the encapsulated and free guests and the integrals of selected protons of **4b** in the NMR spectra of solutions containing known amounts of **4b** and guest (Table III). Determination of the binding constants K_1 and K_2 for the 1:1 and 2:1 complex formation with (n-C_5H_{11})$_4$NBr by an NMR titration experiment failed. A plot of the binding site saturation S as a function of the added guest concentration is shown in Fig. 5. At low guest concentration, S shows a steep rise, but surprisingly levels off at an approximate saturation of $S = 70\%$, which prevented fitting of the entire dataset to a 2:1 binding model. The origin for the saturation at a lower than expected total occupancy is not fully clear and awaits further experimental studies. One possible explanation might be weak binding of tetrapentylammonium cations to the outside of **4b** similar to our observation in tetraoctylammonium bromide titrations of **4b**. Outside binding could electrostatically decrease the binding affinity of the encapsulated guests.

We rationalise the formation of a 2:1 complex upon addition of (n-C_5H_{11})$_4$NBr to **4b** with the calculated packing coefficients PC of the 1:1 and 2:1 complexes (Table II). The PCs of self-assembled hydrogen bonding capsules in solution tend to be around 0.55 for neutral guests [63], but may be higher in the

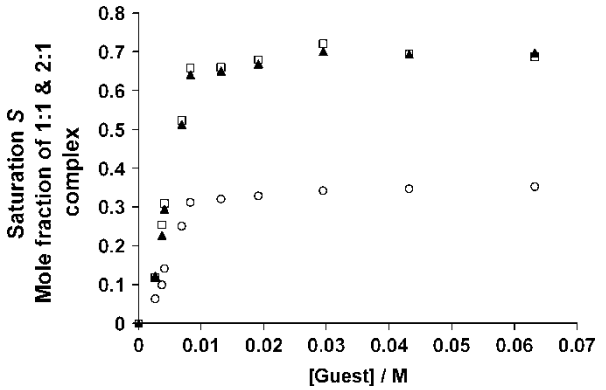

FIGURE 5 Binding isotherm for the encapsulation of (n-C_5H_{11})$_4$NBr inside **4b** in THF-d_8 at −5°C showing saturation of binding sites S ($0 \le S \le 1$; ▲), mole fraction of **4b**⊙(n-C_5H_{11})$_4$NBr (□) and mole fraction of **4b**⊙2(n-C_5H_{11})$_4$NBr) (○) as a function of the guest concentration.

complexes with quaternary ammonium guests or in the solid state [62]. In the case of **4b**, encapsulation of the second (n-$C_5H_{11})_4$NBr guest changes the PC from an unfavourable 0.31 to a close to the ideal value of 0.61 [62b,d, 63]. Since proper space occupancy is often associated with a high complex stability [63], the stability gain associated with the ideal packing in the 2:1 complex could easily compensate for possible electrostatic repulsion between the ammonium ions, which destabilises the 2:1 complex.

In THF-d_8, the stability constant K_1 of the 1:1 complexes decreases in the order K_1(n-$C_7H_{15})_4$NBr) > K_1(n-$C_6H_{13})_4$NBr) ≫ (K_1(n-$C_8H_{17})_4$NBr) (Table III). The stronger binding of (n-$C_7H_{15})_4$NBr when compared with the smaller and larger binding of (n-$C_6H_{13})_4$NBr and (n-$C_8H_{17})_4$NBr can be rationalised with better size and shape complementarities between (n-$C_7H_{15})_4N^+$ and cavity of **4b** (Fig. 6). In space-filling models, each CH_3 group of (n-$C_7H_{15})_4N^+$ in its fully extended conformation can properly CH–π-interact with a cavitand. This guest orientation is qualitatively supported by the Complexation-induced shift, which, for the guest's methyl protons, is close to the maximum value $\Delta\delta \sim 4$–4.5 observed in the cavitand-based container molecules and which steadily decreases further along the chain (Table II) [64–66]. For (n-$C_6H_{13})_4N^+$, penetration of the CH_3 groups in the cavitands is inferior (Fig. 6A). Accommodation of (n-$C_8H_{17})_4N^+$ requires several *gauche* conformations raising the guest's conformational energy, which may be the reason for the absence of complexation despite a good cavity occupation in hypothetical **4b**⊙(n-$C_8H_{17})_4$NBr (PC = 0.47; Fig. 6C).

Solvent has a substantial influence on the stability of **4b**⊙(n-$C_7H_{15})_4$NBr, suggesting that desolvation of the cavity of **4b** and the guest is a major driving force for complexation. No complexation was observed in $CDCl_3$. On the other hand, the free energy of complexation ΔG_{compl} is ~2 kcal/mol more negative in toluene-d_8 when compared with THF-d_8. Furthermore, binding was entropy driven and enthalpy opposed in the former and enthalpy driven and entropy opposed in the latter solvent (Table III).

We explain this with the different strength of solvent–host and solvent–guest interactions and the compensating enthalpy and entropy contributions to ΔG_{compl} as the solvent is released during guest binding [67]. Stronger host–solvent and guest–solvent intermolecular forces are expected for toluene, in the form of cation–π interactions with (n-$C_7H_{15})_4N^+$ and CH-π- and π-stacking interactions with cavitands and linker aryl units of **4b**. They will lead to a higher order of the solvation shell when compared with THF. Thus, release of the toluene solvation shell upon complexation of (n-$C_7H_{15})_4N^+$ will favourably contribute to the entropy of complexation, but unfavourably to enthalpy of complexation.

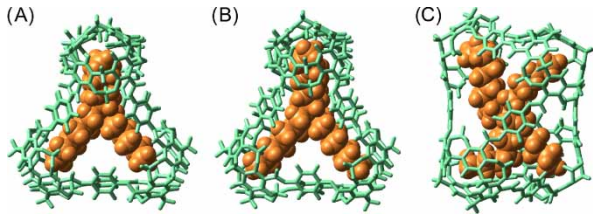

FIGURE 6 Energy-minimised space-filling models of **4b**⊙(n-$C_6H_{13})_4N^+$ (A), **4b**⊙(n-$C_7H_{15})_4N^+$ (B) and **4b**⊙(n-$C_8H_{17})_4N^+$ (C) (MM3 (*60*), gas phase). Colouring: **4b** aquamarine; guest orange.

CONCLUSIONS

We have demonstrated several new examples of one-pot multicomponent nanocapsule syntheses using DCC, which complement earlier thermodynamically controlled polyimino nanocapsule syntheses. Here, we show that cavitand **2** inherently favours the formation of spherical 4:8 assemblies **4b–d**, if condensed with rigid linear diamines, such as 1,4-phenylenediamine **3b**, benzidine **3c** or 4,4′-ethylenedianiline **3d**. These nanocapsules have the shape of a tetragonal tetrahedron. Furthermore, we have shown that nanocapsule **4b** binds one medium-sized tetraalkylammonium bromide and also forms complexes with two guests, if an optimal space occupancy inside the capsule results [63]. Water-soluble derivatives are expected to show interesting binding properties owing to their spacious cavities with volumes greater than 1200 Å^3 and their expected rigidity, which should prevent a hydrophobic collapse in water. We are currently pursuing this direction.

The formation of tetragonal tetrahedra is reminiscent of the coordination chemistry of cavitands bearing four dithiocarbamate ligands, which upon addition of Cu^{2+} assemble into a related tetrahedral coordination capsule [68]. We explain the preference of tetragonal hexadecaiminotetrahedra formation with the structural features of the cavitand building block and the angles between C_{aryl}—$C_{carbonyl}$ bonds, which are more suitable to yield a tetragonal tetrahedron and which would induce strain in the 6:12 octahedral or 8:16 square antiprismatic assemblies. Thus, some conformational flexibility in the X group of a linear diamine H_2N-X-NH_2 is needed to form the latter structures, which is the case for ethylene-1,2-diamine [53]. Nevertheless, hexameric nanocapsules can be assembled through an alternative strategy using rigid trigonal planar triamines as the polyamino building block [69].

Finally, from this and earlier nanocapsule syntheses using tetraformylcavitands, three general

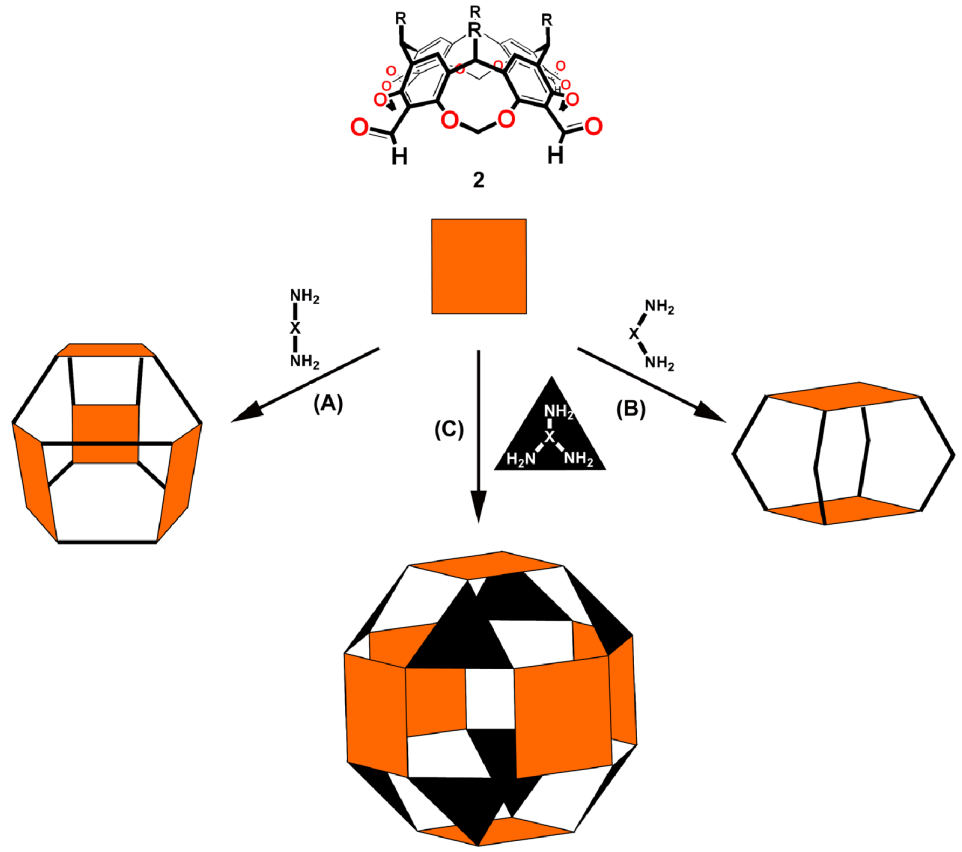

SCHEME 2 Rational design of cavitand nanocapsules.

guidelines for the rational design of polyimino nanocapsules emerge (Scheme 2):

1. Condensation with rigid linear diamines H_2N-X-NH_2 yields tetragonal tetrahedra (Scheme 2A).
2. Condensation with a diamines, whose C—N bonds form a 120° angle, yields octaimine hemicarcerands (Scheme 2B) [51, 52].
3. Condensation with a rigid trigonal planar triamine yields a rhombicuboctahedral nanocapsule (Scheme 2C) [69].

We believe that more guidelines can be added to this list once other polyformyl building blocks have been tested and may yield new nanocapsule geometries that formally belong to the families of Archimedean and Platonic solids [4]. Work along this line is in progress in this laboratory.

Acknowledgements

We thank the National Science Foundation for support of this research (Grant CHE-0518351).

References

[1] Cram, D. J.; Cram, J. M. *Container Molecules and Their Guests*; Royal Society of Chemistry: Cambridge, UK, 1994.
[2] Jasat, A.; Sherman, J. C. *Chem. Rev.* **1999**, *99*, 931.
[3] Warmuth, R.; Yoon *J. Acc. Chem. Res.* **2001**, *34*, 95.
[4] MacGillivray, L. R.; Atwood, J. L. *Angew. Chem. Int. Ed. Engl.* **1999**, *38*, 1018.
[5] Fujita, M.; Tominaga, M.; Hori, A.; Therrien, B. *Acc. Chem. Res.* **2005**, *38*, 371.
[6] Rebek, J. Jr. *Angew. Chem.* **2005**, *44*, 2068.
[7] Rebek, J. Jr. *Chem. Soc. Rev.* **1996**, *25*, 255.
[8] Warmuth, R. J. *Incl. Phenom.* **2000**, *37*, 1.
[9] Lützen, A. *Angew. Chem. Int. Ed.* **2005**, *44*, 1000.
[10] Cram, D. J.; Tanner, M. E.; Thomas, R. *Angew. Chem. Int. Ed. Engl.* **1991**, *30*, 1024.
[11] Warmuth, R. *Angew. Chem. Int. Ed. Engl.* **1997**, *36*, 1347.
[12] Warmuth, R. *J. Am. Chem. Soc.* **2001**, *123*, 6955.
[13] Liu, X.; Chu, G.; Moss, R. A.; Sauers, R. R.; Warmuth, R. *Angew. Chem. Int. Ed. Engl.* **2005**, *44*, 1994.
[14] Ziegler, M.; Brumaghim, J. L.; Raymond, K. N. *Angew. Chem. Int. Ed. Engl.* **2000**, *39*, 4119.
[15] Makeiff, D. A.; Vishnumurthy, K.; Sherman, J. C. *J. Am. Chem. Soc.* **2003**, *125*, 9558.
[16] Kang, J.; Rebek, J. Jr. *Nature* **1996**, *385*, 50.
[17] Fiedler, D.; Bergman, R. G.; Raymond, K. N. *Angew. Chem. Int. Ed.* **2004**, *43*, 6748.
[18] Warmuth, R.; Kerdelhué, J.-L.; Sánchez Carrera, S.; Langenwalter, K. J.; Brown, N. *Angew. Chem. Int. Ed. Engl.* **2002**, *41*, 96.
[19] Yoshizawa, M.; Takeyama, Y.; Kusukawa, T.; Fujita, M. *Angew. Chem. Int. Ed. Engl.* **2002**, *41*, 1347.
[20] Warmuth, R.; Maverick, E. F.; Knobler, C. B.; Cram, D. J. *J. Org. Chem.* **2003**, *68*, 2077.
[21] Yoshizawa, M.; Tamura, M.; Fujita, M. *Science* **2006**, *312*, 251.
[22] Pagba, C.; Zordan, G.; Galoppini, E.; Piatnitski, E. L.; Hore, S.; Deshayes, K.; Piotrowiak, P. *J. Am. Chem. Soc.* **2004**, *126*, 9888.
[23] Menozzi, E.; Pinalli, R.; Speets, E. A.; Ravoo, B. J.; Dalcanale, E.; Reinhoudt, D. N. *Chem. Eur. J.* **2004**, *10*, 2199.
[24] Gibb, C. L. D.; Gibb, B. C. *J. Am. Chem. Soc.* **2004**, *126*, 11408.
[25] Mough, S. T.; Goeltz, J. C.; Holman, K. T. *Angew. Chem. Int. Ed.* **2004**, *43*, 5631.

[26] Yoshizawa, M.; Kumazawa, K.; Fujita, M. *J. Am. Chem. Soc.* **2005**, *127*, 13456.
[27] Rechavi, D.; Scarso, A.; Rebek, J. Jr. *J. Am. Chem. Soc.* **2004**, *126*, 7738.
[28] Yamanaka, M.; Rebek, J. Jr. *Chem. Commun.* **2004**, 1960.
[29] Wyler, R.; de Mendoza, J.; Rebek, J. Jr. *Angew. Chem. Int. Ed. Engl.* **1993**, *32*, 1699.
[30] MacGillivray, L. R.; Atwood, J. L. *Nature* **1997**, *389*, 469.
[31] Prins, L. J.; Huskens, J.; De Jong, F.; Timmerman, P.; Reinhoudt, D. N. *Nature* **1999**, *398*, 498.
[32] Prins, L. J.; De Jong, F.; Timmerman, P.; Reinhoudt, D. N. *Nature* **2000**, *408*, 181.
[33] Ugono, O.; Holman, K. T. *Chem. Commun.* **2006**, 2144.
[34] Gerkensmeier, T.; Iwanek, W.; Agena, C.; Fröhlich, R.; Kotila, S.; Näther, C.; Mattay, J. *Eur. J. Org.* **1999**, *9*, 2257.
[35] Fujita, M.; Oguro, D.; Miyazawa, M.; Oka, H.; Yamaguchi, K.; Ogura, K. *Nature* **1995**, *378*, 469.
[36] Beissel, T.; Power, R. E.; Raymond, K. N. *Angew. Chem. Int. Ed. Engl.* **1996**, *35*, 1084.
[37] Olenyuk, B.; Whiteford, J. A.; Fechtenkoetter, A.; Stang, P. J. *Nature* **1999**, *398*, 796.
[38] Olenyuk, B.; Levin, M. D.; Whiteford, J. A.; Shield, J. E.; Stang, P. J. *J. Am. Chem. Soc.* **1999**, *121*, 10434.
[39] Ziegler, M.; Davis, A. V.; Johnson, D. W.; Raymond, K. N. *Angew. Chem. Int. Ed. Engl.* **2003**, *42*, 665.
[40] Tominaga, M.; Suzuki, K.; Murase, T.; Fujita, M. *J. Am. Chem. Soc.* **2005**, *127*, 11950.
[41] Rowan, S. J.; Cantrill, S. J.; Cousins, G. R. L.; Sanders, J. K. M.; Stoddart, J. F. *Angew. Chem. Int. Ed. Engl.* **2002**, *41*, 898.
[42] Lehn, J.-M. *Chem. Eur. J.* **1999**, *5*, 2455.
[43] Corbett, P. T.; Leclaire, L.; Vial, J.; West, K. R.; Wietor, J.-L.; Sanders, J. K. M.; Otto, S. *Chem. Rev.* **2006**, *106*, 3652.
[44] Giuseppone, N.; Schmitt, J.-L.; Lehn, J.-M. *Angew. Chem. Int. Ed. Engl.* **2004**, *43*, 4902.
[45] Chow, C.-F.; Fujii, S.; Lehn, J.-M. *Angew. Chem. Int. Ed. Engl.* **2007**, *46*, 5007.
[46] Giuseppone, N.; Fuks, G.; Lehn, J.-M. *Chem. Eur. J.* **2006**, *12*, 1723.
[47] Skene, W. G.; Lehn, M. *PMSE Preprints* **2004**, *91*, 943.
[48] Chichak, K. S.; Cantrill, S. J.; Pease, A. R.; Chiu, S.-H.; Cave, G. W. V.; Atwood, J. L.; Stoddart, J. F. *Science* **2004**, *304*, 1308.
[49] Wang, L.; Vysotsky, M. O.; Bogdan, A.; Bolte, M.; Bohmer, V. *Science* **2004**, *304*, 1312.
[50] Pentecost, C. D.; Peters, A. J.; Chichak, K. S.; Cave, G. W. V.; Cantrill, S. J.; Stoddart, J. F. *Angew. Chem. Int. Ed. Engl.* **2006**, *45*, 4099.
[51] Ro, S.; Rowan, S. J.; Pease, A. R.; Cram, D. J.; Stoddart, J. F. *Org. Lett.* **2000**, *2*, 2411.
[52] Quan, M. L. C.; Cram, D. J. *J. Am. Chem. Soc.* **1991**, *113*, 2754.
[53] Liu, X.; Warmuth, R. *J. Am. Chem. Soc.* **2006**, *128*, 14120.
[54] Liu, X.; Liu, Y.; Li, G.; Warmuth, R. *Angew. Chem. Int. Ed. Engl.* **2006**, *45*, 901.
[55] Liu, X.; Warmuth, R. *Nature Protocols* **2007**, *2*, 1288.
[56] Quan, M. L. C.;, PhD Thesis, University of California at Los Angeles, 1990, Chapter III, 93.
[57] Wu, D.; Chen, A.; Johnson, Jr, C. S. *J. Magn. Reson. A* **1995**, *115*, 260.
[58] Riddick, J. A., Bunger, W. B., Sakano, T. K., Eds.; Organic Solvents, 4th ed.; Wiley-Interscience: New York, 1986.
[59] Holz, M.; Mao, X.; Seiferling, D. *J. Chem. Phys.* **1996**, *104*, 669.
[60] Allinger, N. L.; Yuh, Y. H.; Lii, J-H. *J. Am. Chem. Soc.* **1989**, *111*, 8551.
[61] The cavity volume was calculated with the program *DeepView/Swiss Pdb-Viewer* (Guex, N.; Peitsch, M.; Schwede, T.; Diemand, A. *DeepView/Swiss Pdb-Viewer*, Version 3.7, Glaxo Smith Kline).
[62] For encapsulation of tetraalkylammonium cations in other molecular capsules see also: (a) Shivanyuk, A.; Rebek, J., Jr. *PNAS*, **2001**, *98*, 7662. (b) Shivanyuk, A.; Friese, J. C.; Doering, S.; Rebek, J. Jr. *J. Org. Chem*. **2003**, *68*, 6489. (c) Yamanaka, M.; Shivanyuk, A.; Rebek, J. Jr., *J. Am. Chem. Soc.* **2004**, 126, 2939. (d) Vysotsky, M. O.; Pop, A.; Broda, F.; Thondorf, I.; Boehmer, V. *Chem. Eur. J.* **2001**, *7*, 4403. (e) Shivanyuk, A.; Paulus, E. F.; Rissanen, K.; Kolehmainen, E.; Boehmer, V., *Chem. Eur. J.* **2001**, *7*, 1944. (f) Ahman, A.; Luostarinen, M.; Rissanen, K.; Nissinen, M. *New J. Chem.* **2007**, *31*, 169. (g) Caulder, D. L.; Powers, R. E.; Parac, T. N.; Raymond, K. N. *Angew. Chem. Int. Ed. Engl.* **1998**, *37*, 1840.
[63] Mecozzi, S.; Rebek, J. Jr. *Chem. Eur. J.* **1998**, *4*, 1016.
[64] Robbins, T. A.; Knobler, C. B.; Bellew, D. R.; Cram, D. J. *J. Am. Chem. Soc.* **1994**, *116*, 111.
[65] Makeiff, D. A.; Pope, D. J.; Sherman, J. C. *J. Am. Chem. Soc.* **2000**, *122*, 1337.
[66] Liu, Y.; Warmuth, R. *Angew. Chem. Int. Ed. Engl.* **2005**, *44*, 7107.
[67] Cram, D. J.; Choi, H.-J.; Bryant, J. A.; Knobler, C. B. *J. Am. Chem. Soc.* **1992**, *114*, 7748.
[68] Fox, O. D.; Drew, M. G. B.; Beer, P. D. *Angew. Chem. Int. Ed. Engl.* **2000**, *39*, 135.
[69] Liu, Y.; Liu, X.; Warmuth, R. *Chem. Eur. J.*, **2007**, *13*, 8953.
[70] Warmuth, R.; Maverick, E. F.; Knobler, C. B.; Cram, D. J. *J. Org. Chem.* **2003**, *68*, 2077.